INTERNATIONAL JOURNAL OF AUTOMOTIVE AND MECHANICAL ENGINEERING
ISSN: 2229-8649 e-ISSN: 2180-1606
VOL. 20, ISSUE 3, 2023, 10671 –10683
DOI: https://doi.org/10.15282/ijame.20.3.2023.10.0824

RESEARCH ARTICLE

Performance Analysis and Optimization of Regenerative Gas Turbine Power Plant using RSM

M. Bensouici[1,*], M. W. Azizi[1] and F. Z. Bensouici[2]

[1]Department of Mechanical and Electromechanical, Institute of Sciences and Technology, University Center of Mila, Mila 43000, Algeria
[2]Faculty of Pharmaceutical Process Engineering, University of Constantine 3, UVN05, Ali Mendjeli N V, Khroub, Constantine 25000, Algeria

ABSTRACT - In the present study, a thermodynamic analysis of thermal performance is carried out in a regenerative GT power plant. The optimization procedure of design parameters is realized by the response surface methodology (RSM). The thermodynamic simulations were carried out using the EES code for numerous variables such as compression ratio ($2 \leq r_p \leq 12$), inlet temperature ($273 \leq T_1 \leq 313$K), turbine inlet temperature ($1200 \leq T_3 \leq 1600$K), and regenerator effectiveness ($45 \leq \varepsilon \leq 85$%). Analysis of variance (ANOVA) was carried out to identify the process parameters that influence thermal efficiency (η_{th}) and specific fuel consumption (SFC). Then, a second-order regression model was developed to correlate the process parameters with η_{th} and SFC. Consequently, numerical and graphical optimizations were performed to achieve multi-objective optimization for the desired criteria. According to the desirability function approach, it can be seen that the optimum objective functions are η_{th}=50.61% and SFC=0.117 kg/kWh, corresponding to process parameters T_1=273.26K, T_3=1597.64K, r_p=6.95 and ε=84.89%. Lastly, verification simulations were conducted to validate the importance of the generated statistical models.

ARTICLE HISTORY

Received	:	28th Oct 2022
Revised	:	12th Sept 2023
Accepted	:	25th Sept 2023
Published	:	09th Oct 2023

KEYWORDS

Thermodynamic analysis;
Optimization;
Regenerative gas turbine;
Power plant;
Performance

1.0 INTRODUCTION

Electrical energy is a crucial aspect of the economic growth of all nations worldwide. Its proportional significance grows with technological advancement, industrialization, and the desire for contemporary comfort. Increasing its output is connected with enhancing the quality of life and producing riches. Electricity generation is a vital indication that affects growth disparities in various areas of the world. The gas turbine is the essential element of a power plant. It is a rotary engine that turns the burned gas energy into mechanical energy, which is turned into electrical energy. The main factors that impact gas turbine effectiveness are compression ratio, turbine intake and exhaust temperature, isentropic compressor and turbine efficiency, air humidity, and ambient temperature [1-4]. El Hadik [5] studied the atmospheric conditions influence, such as ambient temperature, pressure, and relative humidity on GT performances (ambient temperature (20-60°C), altitude (0- 2000 m above sea level), and relative humidity (0- 100 %). Among these three parameters, he found that the ambient temperature dramatically affects the efficiency and net work of GT. Badran [6] discussed the parameters that improve gas turbine performances. It found that the compressor and turbine efficiencies, pressure ratio, and turbine inlet temperature strongly affect the GT characteristics. Also, greater turbine-inlet temperatures raise the net work generation of the cycle and enhance the cycle performance.

In order to increase the ambient air density entering the compressor due to the high ambient temperature to increase the air mass flow rate and improve the power of the gas turbine, the ambient air is cooled using several methods. El-Shazly et al. [7] studied the comparison between evaporative cooling and absorption chillers. They stated that the GT with an absorption chiller and regenerator is the optimum option with the maximum output power, thermal effectiveness, and reduced energy expenditures. Alhazmy and Najjar [8] investigated two distinct kinds of air coolers. They found that spray coolers boost the GT efficiency in a significantly less expensive manner than the cooling coils. Several gas turbine refinement techniques have been used, such as regeneration, reheating, and intercooling. Omar et al. [9] studied the efficiency of the regenerative GT. They found that increasing regeneration efficiency or compression ratio increases net mechanical work, and increasing ambient air temperature decreases thermal efficiency. Ahmed and Tariq [10] presented a study of a regenerative and intercooled GT. The results show that the compression ratio, temperature of the inlet compressor and turbine played a very vital role in the overall performance of a regenerative and intercooled gas turbine. Alfellag [11] conducted a thermodynamic study of GT with intercooling, reheating and regeneration. It found that thermal efficiency increases with increasing intercooler and regenerator efficiency, reheat temperature, turbine and compressor efficiencies and decreasing ambient temperature. The decrease in ambient regeneration It found that thermal effectiveness rises with increasing exchanger and regenerator efficiency, reheat temperature, turbine and compressor efficiencies, and lower ambient temperature. The drop in ambient temperature, intercooler, and regenerator efficiency reduces specific fuel consumption. The difference between the basic GT and the present design is also shown, and the findings suggest that at any ambient temperature, the efficiency of the suggested design is greater than that of the simple cycle within the range of 16 to 20 %.

*CORRESPONDING AUTHOR | Moumtez Bensouici | ✉ moumtezbensouici1977@gmail.com

Khan and Alzafiri [12] studied five possible combined bottom air cycles parametrically. The filling cycle includes the basic GT cycle, regenerative GT cycle, inter-cool GT cycle, and reheats GT cycle. They found that the combined single-regenerative gas turbine offers maximum net work efficiency and is considered the best cycle simplicity and efficiency compared to other combined cycles. Basha et al. [13] investigated the impact of humidity levels, air inlet temperature, and different kinds of fuel on GT performances. They noticed that net power generation and plant efficiency for natural gas are more significant than for other fuels (diesel and heavy fuel oil). They also observed that turbines operating on propane release substantially fewer carbon dioxide emissions than those running on other fuels. Koç et al. [14] analyzed the characteristics, price of fuel, and emission variables of the primary and recuperative GT cycles with various fuel types. The hydrogen-fueled GT designs' exergy and thermal efficiency were observed to be more significant than those with natural gas-fueled GT designs.

Against the world gas crisis and dependence on electricity and gas, researchers and industrialists are moving towards finding solutions to rationalize electricity consumption and thus rationalize gas consumption. Among the solutions is reducing fuel consumption by the gas turbine by optimizing its energy performance. The performance of optimization approaches in gas turbine power plants has garnered considerable attention in recent years. Several methods, such as the Taguchi method (TM) [15], the genetic algorithm (GA) [16], and the response surface methodology [17], have been employed for the optimization of energy sources. The RSM was employed to analyze and optimize performance characteristics [17]. Moghimi et al. [16] developed a CCHP system using gas turbines, incorporating a dual-pressure HRSG, ST cycle, ERS, and water heater. They optimized the system using a multi-objective genetic algorithm to reduce yearly costs and optimize exergy efficiency. Tang et al. [18] used a genetic algorithm to optimize pressure ratio and efficiency in a small gas turbine. Their study revealed that increasing the overall proportion of pressure and effectiveness by 0.9% and 5.95%, respectively. Naeimi et al. [19] conducted a multi-objective optimization of a CCPP using GA. They treated exergy efficiency, total exergy price, and exergoenvironmental impact as goal criteria. They stated that the heating improved by 11%, 12%, and 32%, respectively. Prajapati et al. [20] performed multi-objective optimization of a combination of Brayton and inverted Brayton cycles to maximize specific work output and minimize thermal efficiency. They found the proposed approach can produce 497 kJ/kg with 44% thermal performance and 464 kJ/kg with 50% efficiency. Mahdavi et al. [21] focussed on optimizing a distinctive CCHP design comprising a GTPP response surface methodology coupled with the TOPSIS approach. The authors stated that maximum net power, minimum system emission, and maximum exergy efficiency are 61.73 MW, 52.87 g/MJ, and 44.22%%, respectively. Ibrahim et al. [22] presented an optimization procedure for GT using RSM. By modifying the pressure proportion and compressor isentropic effectiveness, the optimal thermal efficiency is obtained at 56%. Ibrahim et al. [23] studied the GT thermal performance based on exergy analysis. Their study displays that to ameliorate efficiency, the ambient temperature ought to be decreased, the combustion chamber should have a better air-fuel ratio, and the ability to obtain increased inlet temperature.

Ibrahim et al. [24] conducted a thermodynamic study of integrated GT cycles. They found that higher prevailing thermal efficiency is obtained for regenerative integrated GT. Kazemian and Nassab [25] presented a statistical analysis of the GT cycle using RSM. They proposed the optimal thermal efficiency and net work of cycle, which are 45.71% and 4.182 MW, respectively. Memon et al. [26] conducted a thermo-environmental and financial examination of easy and regenerative GT processes using predictive estimation and optimization according to exergy evaluation. They developed thermodynamic models for both cycles, and they evaluated the exergy destruction rate of other constituents through a parametric study, which included the effects of compressor inlet temperature, turbine inlet temperature, and compressor pressure ratio on gas turbine performance and its environmental impact and cost. From the literature, we note that all the scientific works are limited to parametric studies. Only some works have optimized GT performances and proposed mathematical models or correlations that link the parameters affecting GT performances. In order to enrich this field, we propose a thermodynamic analysis with optimization of the regeneration gas turbine performances utilizing the impact of the following various operating conditions, which are: pressure ratio (r_p), ambient temperature (T_1), inlet turbine temperature (T_3), and effectiveness of regenerator (ε). The RSM is used to obtain appropriate process parameters to produce the highest thermal efficiency with minimal SFC of GT performances.

2.0 THERMODYNAMIC ANALYSIS OF GAS TURBINE WITH REGENERATION

Figure 1 illustrates the structure and its T-S graph of the regenerative gas turbine. In a regenerating gas turbine, the gas temperature exiting the turbine is generally substantially more significant than the air exiting the compressor. Consequently, the elevated pressure air allows the compressor to be reheated by transmitting heating from the warm exhaust gases to it through an opposing current heat exchanger, referred to as a regenerator.

Processes 1-2 and 3-4 are isentropic, $P_2 = P_3$ and $P_4=P_1$. Thus,

$$\frac{T_2}{T_1} = \left(\frac{P_2}{P_1}\right)^{\frac{\gamma_a - 1}{\gamma_a}} = r_p^{\frac{\gamma_a - 1}{\gamma_a}} \tag{1}$$

$$\frac{T_3}{T_4} = \left(\frac{P_3}{P_4}\right)^{\frac{\gamma_a - 1}{\gamma_a}} = \left(\frac{1}{r_p}\right)^{\frac{\gamma_g - 1}{g}} \tag{2}$$

where, $r_p = \frac{P_2}{P_1}$ is the pressure ratio and γ_a, γ_g are the specific heat ratio for air and gases, respectively.

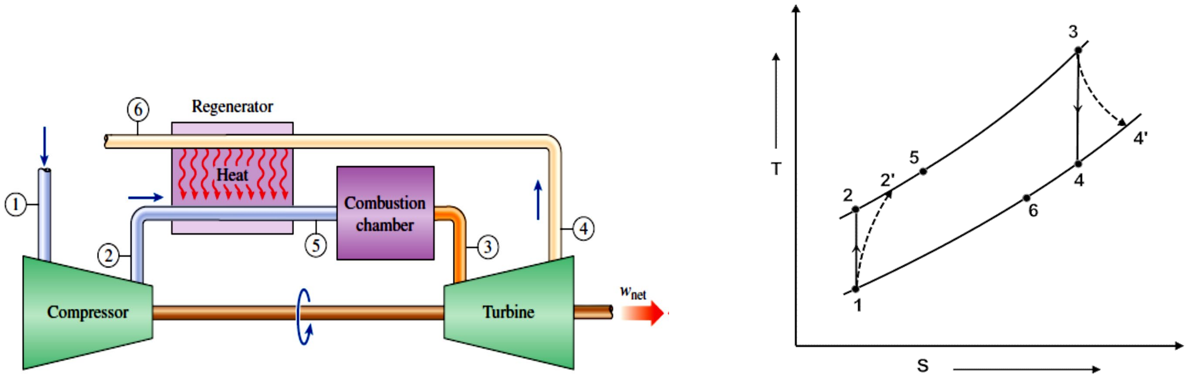

Figure 1. Structure and T-S graph of a regenerative GT

The compressor isentropic efficiency is defined as:

$$\eta_{isc} = \frac{T_2 - T_1}{T_{2'} - T_1} \tag{3}$$

The turbine's isentropic efficiency is described as:

$$\eta_{isc} = \frac{T_3 - T_{4'}}{T_3 - T_4} \tag{4}$$

This equation determines the regenerator's effectiveness:

$$\varepsilon = \frac{T_5 - T_2{}'}{T_4 - T_{2'}} \tag{5}$$

The overall mass flow rate can be obtained by:

$$\dot{m}_g = \dot{m}_a + \dot{m}_f \tag{6}$$

where, $\dot{m}_f$ is the fuel mass flow rate, $\dot{m}_a$ is the air mass flow rate .The air fuel ratio at the combustor is described by:

$$ARF = \frac{\dot{m}_a}{\dot{m}_f} \tag{7}$$

Considering the energy balance in the combustion chamber:

$$\dot{m}_f \, LHV = (\dot{m}_a + \dot{m}_f) C_{pg} \, (T_3 - T_5) \tag{8}$$

where, LHV is the lower heating value of fuel. The following formula defines the work produced by the turbine:

$$W_t = (\dot{m}_a + \dot{m}_f) C_{pg} (T_3 - T_{4'}) \tag{9}$$

The work needed to operate the compressor is represented as:

$$W_c = \dot{m}_a C_{pa} \, (T_{2'} - T_1) \tag{10}$$

The net work of the cycle is given by:

$$W_{net} = W_t - W_c \tag{11}$$

The heat supplied is also expressed by:

$$q_{in} = (\dot{m}_a + \dot{m}_f) C_{pg} (T_3 - T_5) \tag{12}$$

The thermal efficiency is calculated as follows:

$$\eta_{th} = \frac{W_{net}}{q_{in}} \tag{13}$$

The specific fuel consumption (SFC) is determined by:

$$SFC = \frac{3600\ \dot{m}_f}{W_{net}} \tag{14}$$

The previously stated Eqs. (1) to (14) were solved using thermodynamic Engineering Equation code (EES). The values of all the parameters used in this study have been presented in Table 1. Careful selection of particular important parameters is necessary to enhance the thermal performance of a regenerative GTPP for the highest thermal efficiency with minimal specific fuel consumption. The power produced Net of the regenerative gas turbine is in the range of 12.55≤Wnet≤47.14 MW.

Table 1. Operating parameters [1], [4], [9], [12]

S/N	Operating parameters	Value	Unit
1	Mass flow rate of air through compressor ($\dot{m}_a$)	125	kg/s
2	Ambient temperature (T_1)	273-313	K
3	Turbine inlet temperature (T_3)	1200-1600	K
4	Compression pressure ratio (r_p)	2-12	-
5	Lower heating value (LHV) (natural gas, (CH4)	47622	kJ/kg
6	Isentropic efficiency of compressor	80	%
7	Isentropic efficiency of turbine	85	%
8	Regenerator effectiveness	45-85	%
9	Specific heat of air (C_{pa})	1.005	kJ/kg.K
10	Specific heat ratio of air (γ_a)	1.4	-
11	Specific heat of gas (C_{pg})	1.15	kJ/kg.K
12	Specific heat ratio of gas (γ_g)	1.33	-

3.0 RESPONSE SURFACE METHODOLOGY

As a statistical approach, response surface methodology (RSM) optimizes an associated variable as an outcome factor. Distinct input factors modify every outcome variable, where a central-composite design (CCD) is applied here. Also, RSM is employed to enhance and optimize many other thermal engineering structures. It may be used to analyze the influence of various factors on response variables at a cheap cost. RSM uses statistical and mathematical methods to develop an empirical model of subjective characteristics of layout factors. The model is empirically developed via regression from various response values or simulations. The numerical simulation outcomes were evaluated using the outcome of the surface interpolation process utilizing the subsequent second-order polynomial equation [29-31]:

$$y = \beta_0 + \sum_{i=1}^{4} \beta_i x_i + \sum_{i=1}^{4} \beta_{ii} x_i^2 + \sum_{i=1}^{3} \sum_{j=1}^{4} \beta_{ij} x_i x_j \tag{15}$$

where y is the response, and xi and xj are the encoded variables. When adjusted centered approximations (coded levels) are employed for displaying variable levels, b_0, b_i, b_{ii}, and b_{ij} are the average values of results, linear, polynomial, and relationship constant coefficients, respectively. Every variable permitted calculating the variation in the average output per unit rise in x when any additional variables were kept constant. In creating the regression model, the test data were coded based on Eq. (16):

$$x_i = \frac{X_i - X_i^*}{\Delta X_i} \tag{16}$$

where x_i is the i^{th} individual parameter of the empty encoded value, the uncoded value of the i^{th} independent parameter is indicated by X_i^* similarly, at the middle point, the uncoded value of the i^{th} individual parameter is designated by x_{ij}, and the variation in the step value has been described as ΔX_i [31].

3.1 Design of Simulations and Data Collection

In the present work, ambient temperature (T_1), turbine inlet temperature (T_3), pressure ratio (r_p), and regenerator effectiveness (ε) (each at three levels) would serve as distinct factors, as demonstrated in Table 2. All four of these settings were incorporated inside a central composite design (CCD) structure as a frequently employed procedure involving 21 runs. Table 2 shows these variables at their value ranges (low (−1), moderate (0), and high (+1) values). In addition, the η_{th} and SFC are evaluated as reply characteristics. A collection of computational simulations conforming to the CCD design for η_{th} and SFC are provided in Table 3. The statistical analysis was carried out in three parts. For the first time, statistical analysis of variance (ANOVA) was employed to assess the influence of factors and their relationships with the output parameters. The following stage is focused on nonlinear regression to create statistical models displaying the fluctuation of outputs. The final one is employed for optimizing outcomes.

Table 2. Variables and levels of the design parameters

Symbol	Factors	Unit	Level		
			-1	0	+1
T_1	Ambient temperature	K	273	293	313
T_3	Turbine inlet temperature	K	1200	1400	1600
r_p	pressure ratio	-	2	7	12
ε	regenerator effectiveness	%	45	65	85

Table 3. Simulation results for thermal efficiency (ηth) and specific fuel consumption (SFC)

Run, N°	Design parameters				Response parameters	
	T_1 (K)	T_3 (K)	r_p	ε (%)	η_{th} (%)	SFC (kg/kWh)
1	313	1200	2	85	33.73	0.2241
2	293	1200	7	65	32.63	0.2317
3	293	1400	2	65	24.66	0.3066
4	293	1400	12	65	36.27	0.2084
5	293	1400	7	65	37.58	0.2012
6	293	1400	7	65	37.58	0.2012
7	293	1400	7	45	33.36	0.2266
8	273	1400	7	65	39.41	0.1918
9	313	1200	12	85	25.44	0.2972
10	293	1400	7	65	37.58	0.2012
11	293	1400	7	65	37.58	0.2012
12	293	1600	7	65	40.94	0.1847
13	273	1200	2	45	17.87	0.4231
14	273	1600	2	85	40.53	0.1865
15	313	1600	2	45	18.67	0.405
16	313	1400	7	65	35.66	0.212
17	313	1600	12	45	36.36	0.2079
18	273	1600	12	85	47.57	0.1589
19	293	1400	7	65	37.58	0.2012
20	273	1200	12	45	31.3	0.2415
21	293	1400	7	85	43.05	0.1756

3.2 Analysis of Variance

In this investigation, ANOVA is employed to check the prediction's validity. MS, Df, SS, F-value, and P-value are included to check the effectiveness of the calculation. The F-value estimation evaluates the variability of the information about the average error. In addition, the P-values match the hypothesis according to the statistics. Based on the variability estimate, the variables have superior accuracy at F-values bigger than one. To proceed with the ANOVA, the technique of least squares is employed. The findings of this investigation in the form of an ANOVA are provided. The assessment was done at an acceptance rate of 95 %. An ANOVA table is often used to describe the regression equation test and assess the most relevant variables. A "Model F-Value" is produced from a model MS divided by a residual MS. It tests comparing a model variance with an error variance. If the variances have around the same values, the percentage will be near one, and it is less that any of the factors would significantly impact the result. Also, if the "Model P-value" is very low (less than 0.05), the model terms considerably impact the result.

4.0 RESULTS AND DISCUSSION

In the present part, the obtained findings related to influences of design parameters, statistical analysis, mathematical modeling of η_{th} and SFC, and the response surface analysis are presented.

4.1 Code Validation

To give more credibility to our work, the simulation procedure by the EES code was validated with the numerical results of Khan and Tlili [27] and with Poku and Oyinki [28]. For Khan and Tlili [27], a comparison of thermal efficiency as a function of pressure ratio for a simple gas turbine power plant. For Poku and Oyinki [28], a comparison of thermal efficiency as a function of ambient temperature for regenerative GTPP. As shown in Figure 1, it is evident that the current results are in good accord with the results of Khan and Tlili [27] and Poku and Oyinki [28].

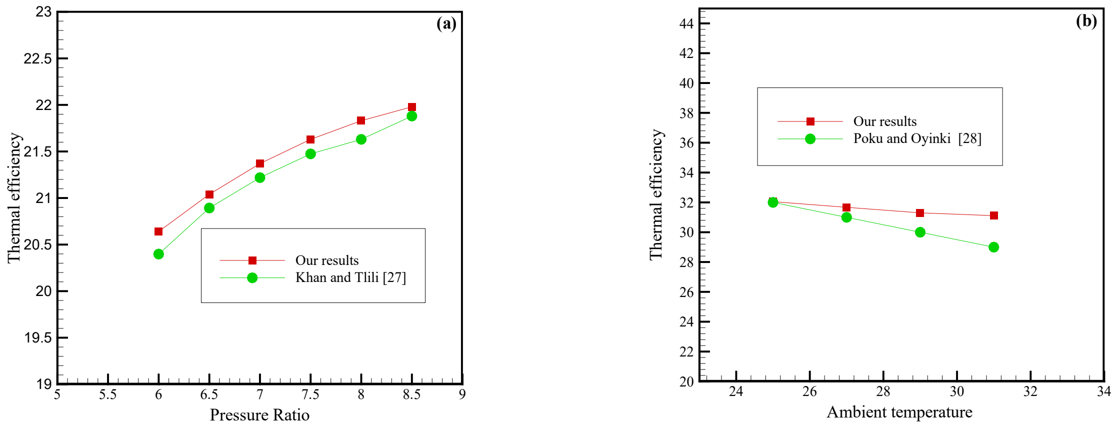

Figure 2. (a) Comparison of thermal efficiency for simple gas turbine between our results and those of Khan and Tlili [27] and (b) Comparison of thermal efficiency for regenerative gas turbine between our results and those of Poku and Oyinki [28]

4.2 Thermal Efficiency Sensitivity According to Design Parameters

Table 3 reports the value of the maximum thermal efficiency (η_{th}), which is achieved with the combination of ambient temperature (T_1), 273K, turbine inlet temperature (T_3), 1600K, pressure ratio (r_p), 12, and regenerator effectiveness (ε), 85%. This maximum thermal efficiency is due to the interaction of pressure ratio (r p) and regenerator effectiveness (ε) on thermal efficiency of the GTPP characterized by the effects of turbine inlet temperature and ambient temperature. The relationship between pressure ratio (r_p) and regenerator effectiveness (ε) is critical to achieving maximum effectiveness. When both r_p and ε are raised concurrently, a balance is established where compression work increases turbine work while decreasing heat input for combustion. This balancing maximizes thermal efficiency by improving heat energy conversion and lowering waste. Additionally, lower ambient temperatures promote efficiency, but higher turbine inlet temperatures raise power production via higher thermal energy for expansion. This result agrees with Ibrahim et al. [22, 24] and Kazemian et al. [25]. The thermal efficiency increases with decreasing ambient temperature in terms of trial conditions.

With the ANOVA test, the least-squares regression approach is applied with the aid of Design Expert Software. The findings of this numerical simulation in the shape of ANOVA are provided. It is an examination that analyzes a term variation with a residual variation. Each of the terms in the model considerably influences the outcome. In Table 4, a "Model F-value" of 66.21 with a "Model P-value" of 0.0001 suggests that the model chosen is essential, and there is only a 0.01% possibility that the "Model F-value" may arise due to noise. The outcomes of the "F-value" effectively show that the pressure ratio (r_p) is the most critical variable contrasted to all variables and that the two-level relationship of pressure ratio and regenerator effectiveness (r_p×ε) was discovered to be the next the greatest significant variable accompanied by quadratic impact r_p^2. This result clearly shows the predominance of the pressure ratio factor on the thermal efficiency compared to other factors.

Table 4. ANOVA results of thermal efficiency (η_{th})

Source	Sum of squares	Df	Mean square	F-value	P-value	Cont. (%)	Remarks
Model	1115.67	14	79.69	66.21	< 0.0001	–	Significant
T_1	7.03	1	7.03	5.84	0.0521	0.62	Not significant
T_3	34.53	1	34.53	28.69	0.0017	3.07	Significant
r_p	172.06	1	172.06	142.96	< 0.0001	15.32	Significant
ε	46.95	1	46.95	39.01	0.0008	4.18	Significant
$T_1 \times T_3$	0.4644	1	0.4644	0.3859	0.5573	0.04	Not significant
$T_1 \times r_p$	15.32	1	15.32	12.73	0.0118	1.36	Significant
$T_1 \times \varepsilon$	0.0601	1	0.0601	0.0499	0.8306	0.0053	Not significant
$T_3 \times r_p$	47.97	1	47.97	39.86	0.0007	4.27	Significant
$T_3 \times \varepsilon$	1.63	1	1.63	1.35	0.2890	0.14	Not significant
$r_p \times \varepsilon$	130.98	1	130.98	108.83	< 0.0001	11.66	Significant
T_1^2	0.2099	1	0.2099	0.1744	0.6908	0.01	Not significant
T_3^2	0.5478	1	0.5478	0.4552	0.5250	0.04	Not significant
r_p^2	117.46	1	117.46	97.60	< 0.0001	10.46	Significant
ε^2	2.34	1	2.34	1.94	0.2129	0.2	Not significant
Residual	7.22	6	1.20	–	–	–	–
Lack of Fit	7.22	2	3.61	–	–	–	Not significant
Pure error	0.0000	4	0.0000	–	–	–	–
Corrected Total	1122.89	20	–	–	–	–	–

Df: degree of freedom, Std. Dev.= 1.10, Mean=34.54, R^2= 99.36%, R^2_{Adj}=97.86%

Ibrahim et al. [24] found that the compression ratio has a strong influence on the overall thermal efficiency, and they also found that the regenerator effectiveness has a positive impact on the improvement of thermal efficiency by using the exhaust gases of the turbine to reduce fuel consumption. Based on the ANOVA findings, it is obvious that the ambient temperature (T_1) on thermal efficiency is not statistically significant, and the variation of thermal efficiency with ambient temperature (T_1) is minimal; however, the effect of pressure ratio, r_p, on thermal efficiency is of statistical impact. The proportion of the impact provides greater clarity for the analysis of the data, which displays that the effect is attributable to the pressure ratio, r_p is 15.32% while the interaction ($r_p \times \varepsilon$) contributes only 11.66% and quadratic effect r_p^2 with a contribution of 10.46%. The result of the minimal influence of ambient temperature on thermal efficiency is in great accord with the outcome of Ibrahim et al. [24].

4.3 Specific Fuel Consumption Sensitivity According to Design Parameters

In Table 3, the SFC was obtained in the range of 0.1589−0.4231kg/kWh. The SFC is impacted mainly through the two-level combination of pressure ratio and regenerator effectiveness ($r_p \times \varepsilon$), pressure ratio, r_p, and the quadratic influence r_p^2, the regenerator effectiveness (ε) having a minor impact on those. The SFC decreases with increasing pressure ratio (r_p) in terms of trial conditions. The results of ANOVA for SFC are reported in Table 5. It can be seen that the ambient temperature (T_1) is not influential on SFC. The findings of the "F-value" effectively show that the relationship between pressure ratio and regenerator effectiveness ($r_p \times \varepsilon$) is determined to be the most important variable impacting the SFC with an impact of 23.14% and that the pressure ratio, r_p, was determined to be the following most crucial variable with a contribution of 19.13% next to the quadratic influence r_p^2 with a contribution of 8.53 %. Figure 3 shows the residual plots for thermal efficiency, η_{th}, and SFC, which provide a visual assessment of the accuracy level of the RSM model. The normal probability of η_{th} and SFC are plotted in Figure 3(a) and 3(b). The residuals are approximately a straight line. Hence, it can be assumed that the deviations are dispersed [32], [33].

Table 5. ANOVA results of specific fuel consumption

	Sum of squares	Df	Mean square	F-value	P-value	Cont. (%)	Remarks
Model	0.0971	14	0.0069	457.25	< 0.0001	–	Significant
T_1	0.0002	1	0.0002	13.45	0.0105	0.20	Significant
T_3	0.0011	1	0.0011	72.84	0.0001	1.13	Significant
r_p	0.0186	1	0.0186	1227.29	< 0.0001	19.13	Significant
ε	0.0013	1	0.0013	85.76	< 0.0001	1.33	Significant
$T_1 \times T_3$	0.0011	1	0.0011	70.51	0.0002	1.13	Significant
$T_1 \times r_p$	0.0009	1	0.0009	59.84	0.0002	0.92	Significant
$T_1 \times \varepsilon$	0.0000	1	0.0000	2.59	0.1590	0	Not significant
$T_3 \times r_p$	0.0017	1	0.0017	111.30	< 0.0001	1.74	Significant
$T_3 \times \varepsilon$	0.0000	1	0.0000	3.11	0.1285	0	Not significant
$r_p \times \varepsilon$	0.0225	1	0.0225	1483.33	< 0.0001	23.14	Significant
T_1^2	5.89E-06	1	5.89E-06	0.3888	0.5559	0.006	Not significant
T_3^2	0.0002	1	0.0002	10.29	0.0184	0.2	Significant
r_p^2	0.0083	1	0.0083	549.27	< 0.0001	8.53	Significant
ε^2	1.32E-06	1	1.32E-06	0.0872	0.7777	0.001	Not significant
Residual	0.0001	6	0.0000	–	–	–	–
Lack of Fit	0.0001	2	0.0000	–	–	–	Not significant
Pure error	0.0000	4	0.0000	–	–	–	–
Corrected Total	0.0972	20	–	–	–	–	–

Cont. (%): Contribution, Std. Dev.= 0.0039, Mean=0.2327, R^2= 99.91%, R^2_{Adj}=99.69%

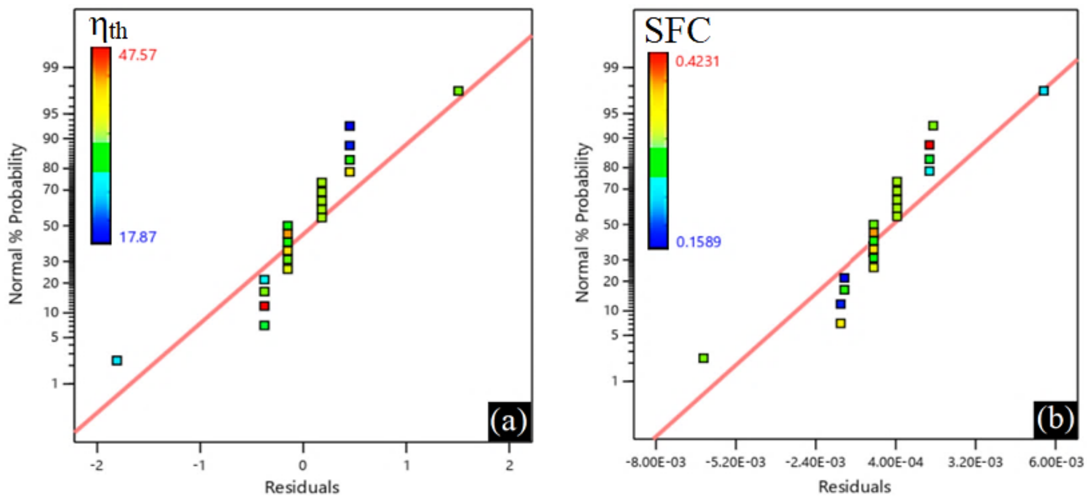

Figure 3. Normal probability plot of residuals for (a) ηth and (b) SFC

4.4 Development of Mathematical Models

Regression models were developed for the η_{th} and SFC using Design Expert Software. The insignificant terms were excluded, except for the main effects. Thus, reduced and improved η_{th} and SFC prediction models were generated. The response variables are the η_{th} and SFC, whereas the predictors are ambient temperature, T_1, turbine inlet temperature, T_3, pressure ratio, r_p, and regenerator effectiveness, ε. Consequently, the adapted equations as a function of actual variables for η_{th} and SFC are presented as follows.

The thermal efficiency, η_{th}, model is given in Eq. (17) with the coefficient of determination, R^2, of 99.36%.

$$\eta_{th} = -14.43 - 0.197T_1 + 0.06T_3 + 7.88r_p + 0.003\varepsilon - 0.014T_1 \times r_p + 0.0025T_3 \times r_p - 0.041r_p \times \varepsilon - 0.27r_p^2 \tag{17}$$

The specific fuel consumption (SFC) model is given in Eq. (18) with the coefficient of determination, R^2, of 99.91%.

$$SFC = +4.27 - 0.012T_1 - 0.0024T_3 - 0.086r_p - 0.007\varepsilon + 6.46E\text{-}06T_1 \times T_3 + 1E\text{-}04T_1 \times r_p - 1.5E\text{-}05T_3 \times r_p + 5.3E\text{-}04r_p \times \varepsilon + 1.95E\text{-}07T_3^2 + 2.28E\text{-}03r_p^2 \tag{18}$$

Figure 4 displays the estimated amounts of η_{th} and SFC from the formulas of the fitting equations and the numerical simulation values. The correlated values reveal a very excellent match for the mathematical equation and may be utilized for exploring the design space. The estimated and adapted R^2 values of η_{th} and SFC were in a good agreement, confirming the proven models' accuracy.

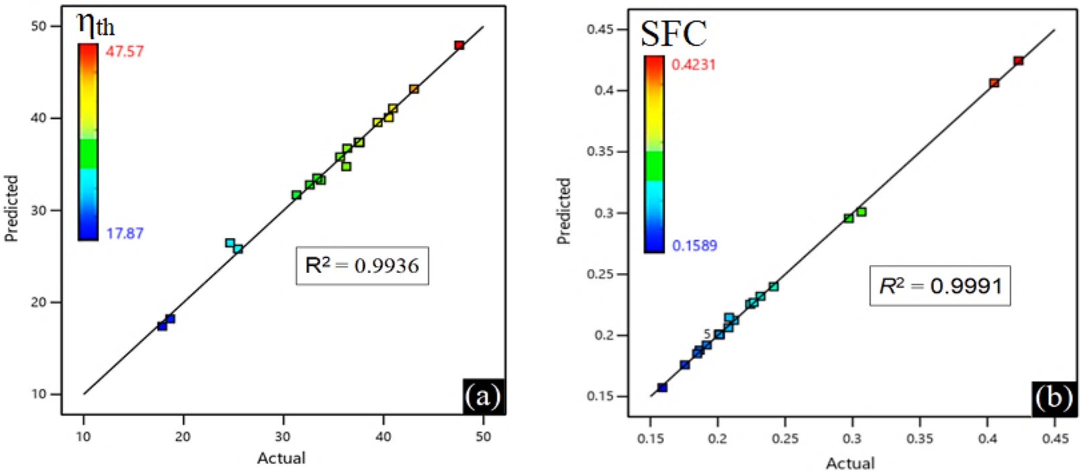

Figure 4. Actual vs. predicted values for (a) η_{th} and (b) SFC

4.5 Response Surface Plots

RSM allows the visualization of a three-dimensional graphic that displays the interaction depending on two variables while maintaining the other variables fixed. The 3D surface plots of different interactions, such as T_1 and T_3, r_p and ε, are presented in Figure 5 for η_{th} and Figure 6 for SFC. Figure 5(a) reveals the influence of ηth with pressure ratio and ambient temperature. It is seen that the pressure ratio has a more substantial influence on thermal efficiency, and its fluctuation is particularly considerable in contrast to other factors at lower ambient temperature values. The maximum η_{th} value obtained was 44% at a pressure ratio of 12 and an ambient temperature of 273 K when the turbine inlet temperature and regenerator effectiveness were fixed at 1600 K and 65%, respectively. Figure 5(b) reveals the influence of η_{th} with pressure ratio and turbine inlet temperature. The η_{th} is considerably high for the higher turbine inlet temperature and pressure ratio value. The best η_{th} value estimated was 45% at a pressure ratio of 10 and the turbine inlet temperature of 1600 K when the ambient temperature and regenerator effectiveness were kept at 273 K and 65%, respectively.

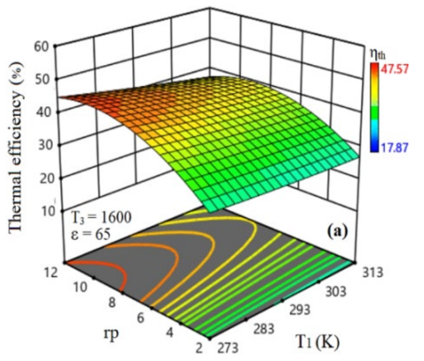

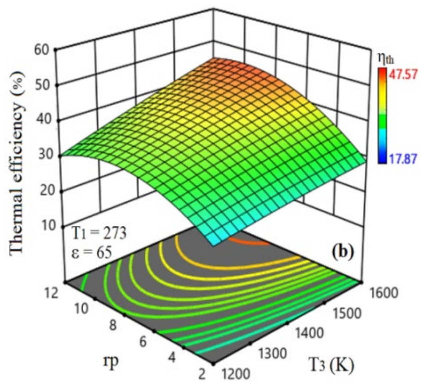

(a) pressure ratio vs ambient temperature (b) pressure ratio vs turbine inlet temperature

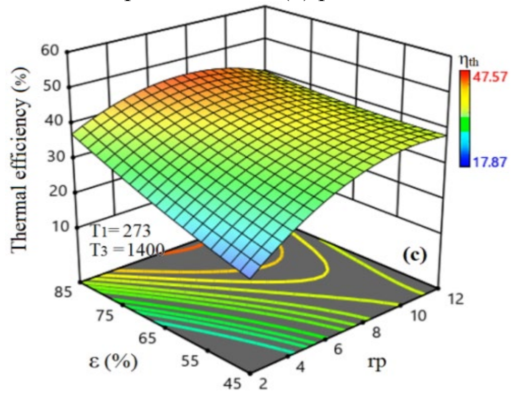

(c) pressure ratio vs regenerator effectiveness

Figure 5. 3D surface plots for the interaction effect of process parameters on thermal efficiency, η_{th}

Figure 5(c) illustrates the estimated response of η_{th} for the corresponding pressure ratio and regenerator effectiveness. It is observed that at the middle values of the pressure ratio, the η_{th} is very high. It is also seen that the decrease in the pressure ratio at low regenerator effectiveness leads to a decrease in η_{th}. The highest η_{th} value predicted was 45% at a pressure ratio of 8 and regenerator effectiveness of 85% when the ambient and turbine inlet temperatures were fixed at 273 K and 1400 K, respectively. Figure 6(a) reveals the influence of SFC on pressure ratio and ambient temperature. It is established that the pressure ratio has the highest impact on SFC. The SFC does not vary much with inlet temperature at a higher pressure ratio range but tends to increase almost with a decreasing pressure ratio at low ambient temperature. The minimum SFC value obtained was 0.2203 at a pressure ratio of 12 and an ambient temperature of 313 K when the turbine inlet temperature and regenerator effectiveness were fixed at 1200 K and 45%, respectively. The effects of the turbine inlet temperature and pressure ratio on SFC are presented in Figure 6(b). It is seen that the pressure ratio has the highest impact on SFC. The SFC is proven to rise by reducing the pressure ratio for all turbine inlet temperature values. The minimum SFC value estimated was 0.1238 at a pressure ratio of 12 and a turbine inlet temperature of 1600 K when the ambient temperature and regenerator effectiveness were fixed at 273 K and 45%, respectively. Figure 6(c) depicts the 3D response behaviour of SFC with pressure ratio and regenerator effectiveness. The SFC is considerably high for lower pressure ratio and regenerator effectiveness. The minimum SFC value obtained was 0.1982 at a pressure ratio of 6 and regenerator effectiveness of 85% when the ambient and turbine inlet temperatures were fixed at 313 K and 1600 K, respectively.

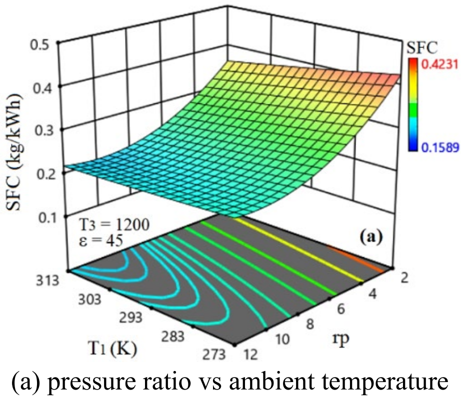

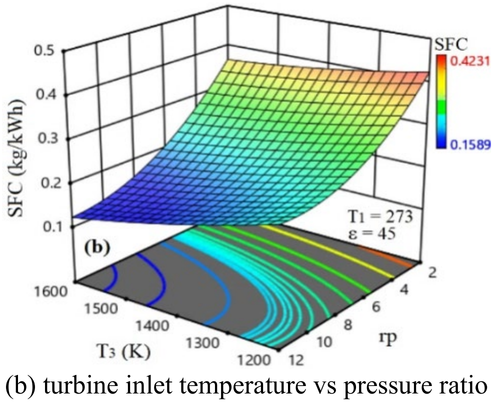

(a) pressure ratio vs ambient temperature (b) turbine inlet temperature vs pressure ratio

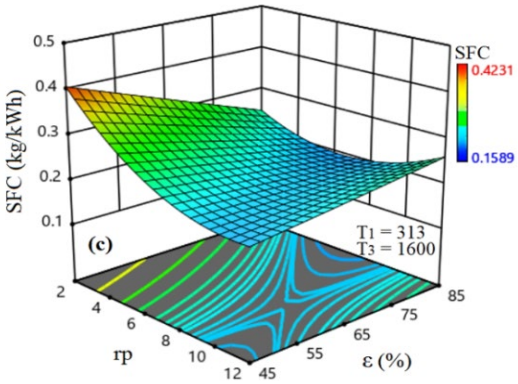

(c) pressure ratio and regenerator effectiveness

Figure 6. 3D surface plots for the interaction effect of process parameters on SFC

4.6 Optimization and Confirmation Simulation

In this part, the findings of the optimization evaluation are exhibited and described in depth. The desire function is a criterion to assess how the parameters optimize a collection of output variables in an interval of 0 to 1. One spotlights the perfect scenario, and 0 demonstrates that several replies are beyond the bounds of their permissible restrictions [34]:

$$DF = \left(\prod_{i=1}^{n} d_i^{wi}\right)^{\frac{1}{\sum_{j-1}^{n} wi}} \tag{19}$$

$$F(x) = -DF$$

where d_i is the desire specified for the ith specified outcome, and w_i is the importance of d_i. For distinct aims for every intended result, the desirability, d_i, is specified in various manners. For an objective to discover a maximum, the desirability is represented as follows:

$$d_i = 0 \; if \; Y_i \le Low_i$$

$$d_i = \left[\frac{Y_i - Low_i}{High_i - Low_i}\right] if \; Low_i \le Y_i \le High_i \tag{20}$$

$$d_i = 1 \; if \; Y_i \ge High_i$$

For an objective to discover a minimum, the desirability is represented as follows:

$$d_i = 1 \; if \; Y_i \le Low_i$$

$$d_i = \left[\frac{High_i - Y_i}{High_i - Low_i}\right] if \; Low_i \le Y_i \le High_i \tag{21}$$

$$d_i = 0 \; if \; Y_i \ge High_i$$

As the Y_i is the noticed value of the i^{th} response variable throughout optimization procedures, the Low_i and the $High_i$ are the smallest and highest values of the simulation results for the i^{th} output. In Eq. (19), w_i is set to one, given that d_i is equally relevant in our investigation. The DF is a coupled desire function [34], and the purpose is to pick an ideal configuration that maximizes the coupled desirability function DF, i.e., minimizing *F(x)*. The restrictions considered throughout the optimization process are listed in Table 6. The most suitable options are provided in Table 7 in order to reduce the desirability level. The desirability value of 1 reflects the smallest value of the SFC with greater η_{th} in the provided range of variables. The outcome of graphic optimization is presented in Figure 7. The graphical optimization plot, referred to as an overlay plot, is a helpful tool where the simulations may be visually explored for the optimal agreement or optimal parameter values by overlaying essential response outlines on a contour chart.

Table 6. Constraints for optimization process

Conditions	Objective	Lower limit	Upper limit	Importance
T_1 (K)	in range	273	313	3
T_3 (K)	in range	1200	1600	3
r_p	in range	2	12	3
ε (%)	in range	45	85	3
η_{th} (%)	Maximized	17.87	47.57	5
SFC (kg/kWh)	Minimized	0.1589	0.4231	5

Table 7. Optimal solutions

N°	T_1 (K)	T_3 (K)	r_p	ε (%)	η_{th} (%)	SFC (kg/kWh)	Desirability	Remarks
1	273.26	1597.64	6.95	84.89	50.61	0.117	1	Selected
2	278.18	1565.13	8.02	84.49	49.35	0.132	1	
3	285.159	1566.67	6.97	84.95	48.17	0.143	1	
4	277.67	1573.71	7.12	80.92	47.99	0.135	0.999	
5	273.28	1568.39	5.45	84.09	47.83	0.134	0.998	
6	284.13	1584.34	6.20	84.08	47.73	0.144	0.997	

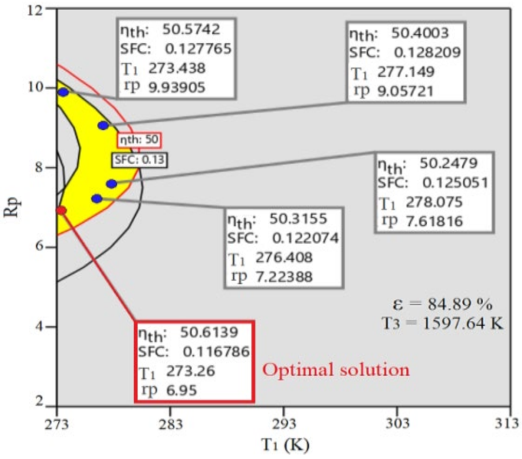

Figure 7. Overlay plot of the most desirable solution

The overlay map displays the "sweet spot" with several output variable locations whose response conditions may be satisfied or needs concurrently match the essential attributes. The contours are drawn at the limitations indicated by the conditions ($50 \leq \eta_{th} \leq 52$ and $0.11 \leq SFC \leq 0.13$). In addition, the graphic optimization illustrates the region of viable answer values in the parameter space in yellow. From this evaluation, it appears that the ambient temperature, T_1, of 273.26K; turbine inlet temperature, T_3, of 1597.64 K, pressure ratio, r_p of 6.95, and regenerator effectiveness, ε of 84.89%, are the optimum values of design parameters while the optimum value thermal efficiency (η_{th}) and specific fuel consumption (SFC) are 50.61% and 0.117 kg/kWh, respectively.

Figure 8 depicts a 2D contour map of the global desire function *D(x)* for the (r_p, T_1) plane where T_3 and ε are set at 1597.64K and 84.89%, respectively. The highest value of function *D(x)*=1 situated close by space colored red around the best solution, suggesting that minor deviations in the vicinity of ambient temperature (T_1), 273.26K; turbine inlet temperature (T_3), 1597.64K, pressure ratio (r_p), 6.95 and regenerator effectiveness (ε), 84.89% are expected not to affect the overall appeal significantly. However, the need to run validation tests at the projected ideal operational settings must be underlined.

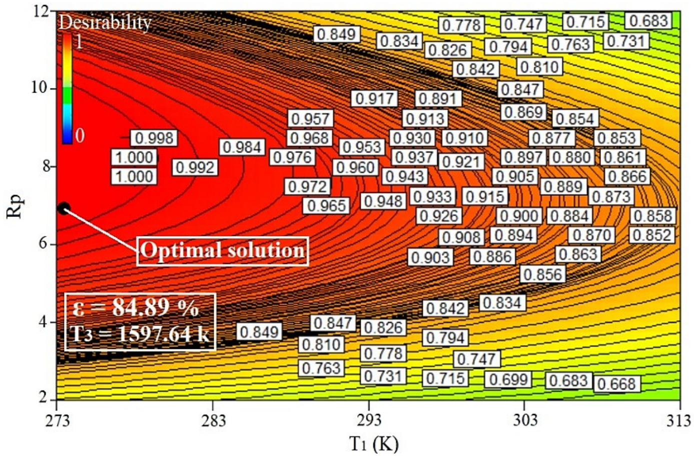

Figure 8. Contour plot of desirability function

The verification simulations were taken out for the optimal state induced by the model for reaching the most increased η_{th} with minimal SFC. The validation trial and their comparisons with the expected values for the η_{th} and SFC are detailed in Table 8. The ratio error between the simulation and the expected significance of η_{th} and SFC lie within 1.64% and 10.68%, respectively. The validation tests are inside the 95% estimation range. The mathematical model produced is excellently well.

Table 8. Validation results of the optimal solution

N°	Design parameters				Thermal efficiency (%)			SFC (kg/kWh)		
	T_1 (K)	T_3 (K)	r_p	ε (%)	Predicted	Actual	Error (%)	Predicted	Actual	Error (%)
1	273.26	1597.64	6.95	84.89	50.61	49.79	1.64	0.117	0.131	10.68

5.0 CONCLUSIONS

In this study, the adoption of RSM on the performance parameters of the GT was performed through the regression models of the η_{th} and SFC to evaluate the impacts of process factors. In order to identify the optimal value of process variables for achieving the best η_{th} with the lowest SFC, the second-order regression model coupled with desirability function optimization was applied. The conclusions collected as a consequence of the research may be stated as follows:

i. Thermal efficiency and specific fuel consumption are considerably impacted by the pressure ratio and the interplay between pressure ratio and regenerator effectiveness (r_p×ε) for all the investigated setups.
ii. Normality checks on the errors of the regression models promise that the methods have retrieved all relevant data from the numerical simulation data, and these tests also confirm the appropriateness of the models.
iii. ANOVA results show that the pressure ratio (r_p), the interaction (r_p×ε) and the quadratic effect r_p^2 affect the thermal efficiency by 15.32%, 11.66% and 10.46%, respectively. The effect of the ambient temperature (T_1) is less significant compared to the other process parameters.
iv. The developed mathematical models are excellently accurate which can be used for predicting thermal efficiency and specific fuel consumption of the GTPP in the limits of the design parameters studied.
v. The desirability function based on multi-response optimization asserted that the optimum value of process parameters to provide the highest η_{th} with minimal SFC are in the region ambient temperature, T_1, of 273.26 K, turbine inlet temperature, T_3 of 1597.64 K, pressure ratio, r_p of 6.95 and regenerator effectiveness, ε, of 84.89% with estimated thermal efficiency of 50.61% and specific fuel consumption of 0.117 kg/kWh.

6.0 ACKNOWLEDGEMENT

The authors gratefully acknowledge the financial support of this work provided by the Algerian Ministry of High Education and Scientific Research. The authors also take this opportunity to express sincere respect to the reviewers for their comments.

7.0 REFERENCES

[1] A. Kumar, A. Singhania, A. K. Sharma, R. Roy and B. K. Mandal, "Thermodynamic analysis of gas turbine power plant," *International Journal of Innovative Research in Engineering & Management*, vol. 4, pp. 648-654, 2017.
[2] A. De Sa and S. Al Zubaidy, "Gas turbine performance at varying ambient temperature," *Applied Thermal Engineering*, vol.31, pp. 2735-2739, 2011.
[3] B. T. Lebele-Alawa and V. Jo-Appah, "Thermodynamic performance analysis of a gas Turbine in an equatorial rain forest environment," *Journal of Power and Energy Engineering,* vol. 3, pp.11-23, 2015.
[4] M. M. Rahman, T. K. Ibrahim, K. Kadirgama, R. Mamat and R. A. Bakar, "Influence of operation conditions and ambient temperature on performance of gas turbine power plant," *Advanced Materials Research*, pp. 189-193, 3007-3013, 2011.
[5] A. A. El Hadik, "The impact of atmospheric conditions on gas turbine performance", *Transactions of the ASME*, vol. 112, pp. 591-596, 1990.
[6] O. O. Badran, "Gas-turbine performance improvements," *Applied Energy*, vol. 64, pp. 263-273, 1999.
[7] A. A. El-Shazly, M. Elhelw, M. M. Sorour, W. M. El-Maghlany, "Gas turbine performance enhancement via utilizing different integrated turbine inlet cooling techniques," *Alexandria Engineering Journal,* vol. 55, pp. 1903-1914, 2016.
[8] M.M. Alhazmy, Y.S.H. Najjar, "Augmentation of gas turbine performance using air coolers," *Applied Thermal Engineering*, vol. 24, pp. 415–429, 2004.
[9] H. Omar, A. Kamel and M. Alsanousi, "Performance of regenerative gas turbine power plant," *Energy and Power Engineering*, vol.9, pp. 136-146, 2017.
[10] A.M. Ahmed, M. Tariq, "Thermal analysis of a gas turbine power plant to improve performance efficiency," *International Journal of Mechanical Engineering and Technology*, vol. 4, pp. 43-54, 2013.
[11] M.A.A. Alfellag, "Parametric investigation of a modified gas turbine power plant," *Thermal Science and Engineering Progress*, vol. 3, pp. 141–149, 2017.
[12] M. N. Khan, and D. Alzafiri, "Air bottoming combined cycle performance analyses by the combined effect of variable parameters," *Archive of Mechanical Engineering,* vol. 69 pp. 497-517, 2022.
[13] M. Basha, S. M. Shaahid, and L. Al-Hadhrami, "Impact of fuels on performance and efficiency of gas turbine power plants," *Energy Procedia*, vol. 14, pp. 558-565, 2012.
[14] Y. Koç¸ H.Yaglı, A. Gorgulu, and A. Koç, "Analyzing the performance, fuel cost and emission parameters of the 50 MW simple and recuperative gas turbine cycles using natural gas and hydrogen as fuel, *International Journal of Hydrogen Energy,* vol. 45, pp. 22138-22147, 2020.
[15] M. E. Elsayed, S. Abdo, A. A. Attia, E. A. Attia, and M. A. Abd Elrahman, "Parametric optimization for the design of gravity energy storage system using Taguchi method," *Scientific Reports,* vol. 12, no. 1, p. 19648, 2022.
[16] M. Moghimi, M. Emadi, P. Ahmadi, and H. Moghadasi, "4E analysis and multi-objective optimization of a CCHP cycle based on gas turbine and ejector refrigeration," *Applied Thermal Engineering,* vol. 141, pp. 516–530, 2018.

[17] D. Tan, Y. Wu, J. Lv, J. Li, X. Ou, *et al.*, "Performance optimization of a diesel engine fueled with hydrogen/biodiesel with water addition based on the response surface methodology," *Energy,* vol. 263, p. 125869, 2023.
[18] Q. Tang, H. Wu, and H. Lou, "Multi-objective optimization of aerodynamic performance for a small single-stage turbine," *Journal of Applied Fluid Mechanics*, vol. 15, no. 5, pp. 1451–1463, 2022.
[19] M. M. Naeimi, M.E. Yazdi, and G. Reza Salehi, "Energy, exergy, exergoeconomic and exergoenvironmental analysis and optimization of a solar hybrid CCHP system," *Energy Sources, Part A, Recovery, Utilization, and Environmental Effects*, vol.32 pp. 1-21, 2019.
[20] P. Prajapati, V. Patel, B.D. Raja, and H. Jouhara, "Thermal efficiency and specific work optimization of combined Brayton and inverse Brayton cycle: a multi-objective approach," *Thermal Science and Engineering Progress,* vol.37, p. 101624, 2022.
[21] N. Mahdavi, P. Mojaver, S. Khalilarya, "Multi-objective optimization of power, CO2 emission and exergy efficiency of a novel solar-assisted CCHP system using RSM and TOPSIS coupled method," *Renewable Energy*, vol. 185, pp. 506–524, 2022.
[22] T. K. Ibrahim, M.M. Rahman, M.K. Mohammed, and F. Basrawi, "Statistical analysis and optimum performance of the gas turbine power plant," *International Journal of Automotive and Mechanical Engineering*, vol. 13, pp. 3215-3225, 2016.
[23] T.K. Ibrahim, F. Basrawi, O. I. Awad, A. N. Abdullah, G. Najafi, *et al.*, "Thermal performance of gas turbine power plant based on exergy analysis," *Applied Thermal Engineering*, vol. 25, pp. 977-985, 2017.
[24] T.K. Ibrahim, M.M. Rahman, and A.N. Abdalla, "Optimum gas turbine configuration for improving the performance of combined cycle power plant," *Procedia Engineering*, vol. 15, pp. 4216 – 4223, 2011.
[25] M. E. Kazemian, and S. A. G. Nassab, "Thermodynamic analysis and statistical investigation of effective parameters for gas turbine cycle using the response surface methodology," *International Journal of Engineering*, vol. 33, pp. 894-905, 2020.
[26] A. G. Memon, K. Harijan, M. A. Uqaili, and R. A. Memon, "Thermo-environmental and economic analysis of simple and regenerative gas turbine cycles with regression modeling and optimization," *Energy Conversion and Management,* vol. 185, pp. 506–524, 2013.
[27] M.N. Khan, and I. Tlili, "New approach for enhancing the performance of gas turbine cycle: A comparative study," *Results in Engineering*, vol. 2, p. 100008, 2019.
[28] R. Poku, and T. Tokoni, "Peformance analysis of a regenerative gas turbine plant modeled with vapour absorption refrigeration system," *Asian Journal of Science and Technology,* vol. 9, no. 9, pp. 8648-8654, 2018.
[29] K. Kumar, and R.K. Verma, "Measurement and evaluation of delamination factors and thrust force generation during drilling of multiwall carbon nanotube (MWCNT) modified polymer laminates," vol. 69, pp. 269–300, 2022.
[30] M.W.Azizi, O. Keblouti, L. Boulanouar and M.A. Yallese, "Design optimization in hard turning of E19 alloy steel by analyzing surface roughness, tool vibration and productivity," *Structural Engineering and Mechanics*, vol. 73, pp. 501–513, 2020.
[31] M. Bensouici, M.W. Azizi, and F.Z. Bensouici, "Multi-objective optimization of mixed convection air cooling in an inclined channel with discrete heat sources," *Structural Engineering and Mechanics*, vol. 79, pp. 51–66, 2021.
[32] D.C. Montgomery, *Design and analysis of experiments,* New York: John Wiley & Sons, 2001.
[33] A. Bouziane, L. Boulanouar, M.W. Azizi, and O. Keblouti, "Analysis of cutting forces and roughness during hard turning of bearing steel," *Structural Engineering and Mechanics*, vol. 66, pp. 285–294, 2018.
[34] R. H. Myers, D. C. Montgomery, "Response surface methodology," *Process and Product*, vol.26 (2), p.798, 2002.